Fiber laser cutting of Ti6Al4V sheets for subsequent welding operations: Effect of cutting parameters on butt joints mechanical properties and strain behaviour

L.D. Scintilla, G. Palumbo, D. Sorgente, L. Tricarico *

Dipartimento di Meccanica, Matematica e Management (DMMM), Politecnico di Bari, Viale Japigia 182, 70126 Bari, Italy

ARTICLE INFO

ABSTRACT

The effect of laser cutting parameters on the mechanical behavior of laser butt welded joints whose edges were obtained by laser cutting was investigated. The paper aims to demonstrate that new high power solid-state fiber lasers not only represent a valid and reliable alternative to the most established CO_2 and Nd:YAG laser sources, but also allow to obtain cuts having edges well suited for subsequent direct laser welding. First Ti6Al4V 1 mm thick sheets having edges machined by milling were laser welded. Once the optimal welding condition was determined, the mechanical characterization of sheets cut by fiber laser and then laser welded was performed. Comparative strain analysis performed by a digital image correlation technique highlighted the effect of the gap between the sheets resulting from the different cut edge quality. Experimental results showed that the correct selection of laser cutting parameters allows to obtain butt joints characterised by mechanical properties comparable with the ones obtained by milling. Cutting edge quality in the optimal range of gap values allows to obtain the best mechanical performances of the joint.

© 2012 Elsevier Ltd. All rights reserved.

1. Introduction

During the last decades, with the escalating fuel prices and awareness of environmental changes more attention is focused in order to develop sustainable products [1]. Their constituent components and structures must be designed, developed and manufactured saving up materials and energy. The use of lightweight alloys is a viable choice in order to achieve sustainability requirements and in particular weight reduction and functional advantages of structures and vehicles that represent the most important goals of the engineering design and manufacturing [2–4]. If compared to the other light alloys, Titanium (Ti) alloys are most widely used for different technologically advanced sectors due to their superior performance characteristics, such as high strength to weight ratio, high corrosion resistance, high strength and stiffness at elevated temperatures, fatigue resistance. Examples are medical, aerospace, automotive, petrochemical, nuclear and power generation industry [5]. The increasingly stringent requirements during operation in these field are met by Ti and its alloys but the elevated raw material and machining costs make their use highly selective, in particular in automotive and aircraft industry. From one side, the high material cost is due to its production by the current Kroll process, which is still quite expensive; anyway, endeavours to reduce the cost of Ti have seen a number of potential alternative production technologies [6]. From the other side, Ti and its alloys cannot be easily manufactured and in a cost-effective way by conventional cutting methods. This is due to their poor thermal conductivity, low elastic modulus and high chemical affinity at elevated temperatures that adversely affect the tools life [7]. High quality components can be produced by forging and subsequent machining, whose costs can be up to 40% of the total costs of a final part [8]. In some cases finished components can have uneconomical buy-to-fly ratios [9].

In order to support the wider use of Ti alloys also in conventional industrial applications and thus reduce the costs associated with the material supply and manufacturing, two main strategies can be adopted.

The first strategy consists in reconsidering the design phase of Ti alloy components in order to optimize the material usage. The production of near-net shape components by a high integrity joining process could significantly reduce the material waste and increase the production rates [9]. Using Tailor welded blanks (TWBs), i.e. welding sheets having different characteristics into a single flat blank before the forming process, is possible to achieve the optimal material arrangement and weight reduction [10,11]. For example, with this manufacturing approach, automakers can add strength to parts where it is needed and reduce the overall weight and cost of a vehicle. TWBs application is expected to be one of the candidates to address also the problem of weight reduction for Ti alloys [12–14].

One of the three approaches for light-weighting illustrated by Mayyas et al. [1], i.e. to develop a design for energy efficiency, is based on the usage of optimized cross-sectional shapes of

* Corresponding author. Tel./fax: +39 080 5962778.
  E-mail address: tricarico@poliba.it (L. Tricarico).

Nomenclature

e_1	major strain	t	sheet thickness (m)
e_2	minor strain	UTS	ultimate tensile strength (N m^{-2})
E_f	elongation to fracture	v_C	cutting speed (m s^{-1})
p	assist gas pressure (Pa)	v_W	welding speed (m s^{-1})
P_L	laser power (W)	x_C	distance from the center of the weld bead in DL
Q	heat input (J m^{-1})		direction (m)
Ra	roughness – arithmetic mean value (m)	YS	yield strength (N m^{-2})
Rt	roughness – total height (m)		

structures. In this way better loading performances are achieved without weight increase using Tailor Welded Blanks/Tubes/Coils (TWB/T/C) technology to customize the blanks thickness and grade according to local performance criteria.

The second strategy consists in modifying the processes used for the Ti alloys components manufacturing and to use advanced processes rather than mechanical cutting methods. Laser cutting is especially indicated because there is no mechanical contact between the workpiece and the cutting tool [15] and the effectiveness of thermal processes depends on the thermal properties of the material to be machined. In this context, laser beam cutting represents a promising process in machining Ti alloy parts. Most papers in literature report results concerning cutting of pure Ti and its alloys using Nd:YAG lasers operating in pulsed mode (PM) [16–18,7] and CO_2 laser operating in continuous wave mode (CW) [19]. Recently, experimental results on CW fiber laser beam cutting of Ti6Al4V alloy thin sheets have been reported [20] for the first time. The advantageous characteristics as power efficiency, beam guidance and beam quality of high-power solid-state disk and fibre lasers, made them valid and reliable alternatives to the CO_2 and Nd:YAG laser sources, as demonstrated by many simulations and experimental results [21–27]. Comparing fiber and CO_2 lasers from a technical and commercial point of view, fiber lasers are better that CO_2 lasers when cutting highly reflective materials and thin section metals (below about 4 mm) [28]. The use of fiber lasers allows to implement the strategy to reduce the manufacturing costs because of the great reduction of processing time. In fact, using CW operation mode allows to obtain a much faster process with respect to the PM. These benefits are of special interest for applications like coil sheet cutting, laser blanking, trimming [29], the integrated cutting and welding with a multifunctional laser combi-head [30] and thus TWB. The possibility to apply laser welding to sheets cut by fiber laser, without the need for further edge machining due to the excellent cut edges quality, reduces the total processing time but makes critical the selection and control of the processing parameters. In fact, in applications with subsequent welding requirements the quality of laser cutting edges is essential for obtaining sound welds in the next manufacturing step [31–33]. Laser beam welding (LBW) is proved to be much more feasible for the production of Ti plate joints since laser welded joints have better combination of strength and ductility with respect to the TIG welding, which represents the most widely used welding methods for Ti alloy [34]. Furthermore LBW provide a significant benefit for obtaining reliable Ti alloy welds due to essential characteristics for TWBs applications like minimum distortion and higher fatigue strength [35–40]. For this kind of applications, an optimization of LBW joint quality based on response surface methodology (RSM) can be required since LBW is used in approximately 99% of all TWBs applications [41]. Anyway, the small values of beam diameter of laser welding process in contrast to hybrid laser-MIG welding make the workpieces and clamping tolerance a critical aspect in order to obtain a reliable joining process.

For this reason, experimental investigation on the effect of fiber laser cutting process parameters on mechanical behaviour of the subsequent Ti6Al4V LBW butt joints was carried out in this work. Once the best Nd:YAG welding parameters on 1 mm thick parts with edges obtained by machining were determined, this condition was used to weld sheets cut with a 2 kW fiber laser varying cutting speed and assist gas pressure. Mechanical characterization of butt joints welds on sheet metal part previously cut with fiber laser was carried out by tensile tests assisted by a digital image correlation (DIC) technique. DIC has been applied in literature to study the local deformative behavior in both formability and tensile tests [2]. In particular, investigations about local tensile properties of weld joints obtained by friction stir [42–48] and laser [49,50] of different metallic materials have been widely reported in literature. Recently DIC was also applied for laser welded Ti-6Al-4V [35,36].

In the present study, DIC technique was used to acquire strain maps in uniaxial tensile tests and to compare the strain behaviour of different types of welded specimens. To the author's knowledge, an experimental analysis concerning the influence of the cut edge quality by the variation of the cutting parameters on the subsequent laser welding of Ti6Al4V alloy sheets with fiber laser, has not been performed. The final aim is to detect the laser cutting process parameter window that allows to obtain edges well suited for subsequent direct laser welding process, i.e. that produces butt joints with mechanical properties comparable with the ones obtained by milling. The acquisition of a detailed level of knowledge about laser cutting and subsequent welding phase was obtained.

2. Experimental details

Cutting and welding experiments were performed on the as-received alpha–beta alloy Ti6Al4V (grade 5) sheets 1 mm thick. Sheets were characterised by a nominal composition of 5.50–6.75 wt% Al, 3.50–4.50 wt% V, <0.4 wt% Fe, balance Ti. The experiments were performed in three distinct phases illustrated in Fig. 1.

The objective of the first phase was the establishment of the best operating welding condition basing on tensile tests. In this case welding tests were performed on sheets with milling machined edges. In the second phase the effect of the cutting speed and the assist gas pressure on the quality of sheet edges cut by fiber laser was evaluated by means of roughness measurements. The final phase of experiments combines previous results: butt joints were thus realized with the best operating condition previously determined welding sheets whose edges were obtained varying the laser cutting parameters. In this case, mechanical characterization performed by tensile tests was realized in combination with a strain analysis performed using a DIC system. The present section describes the experimental procedures and the process settings used.

2.1. Butt joint welding tests

As regards the join operations, the experimental settings were kept unchanged during the two main experimental phases: the re-
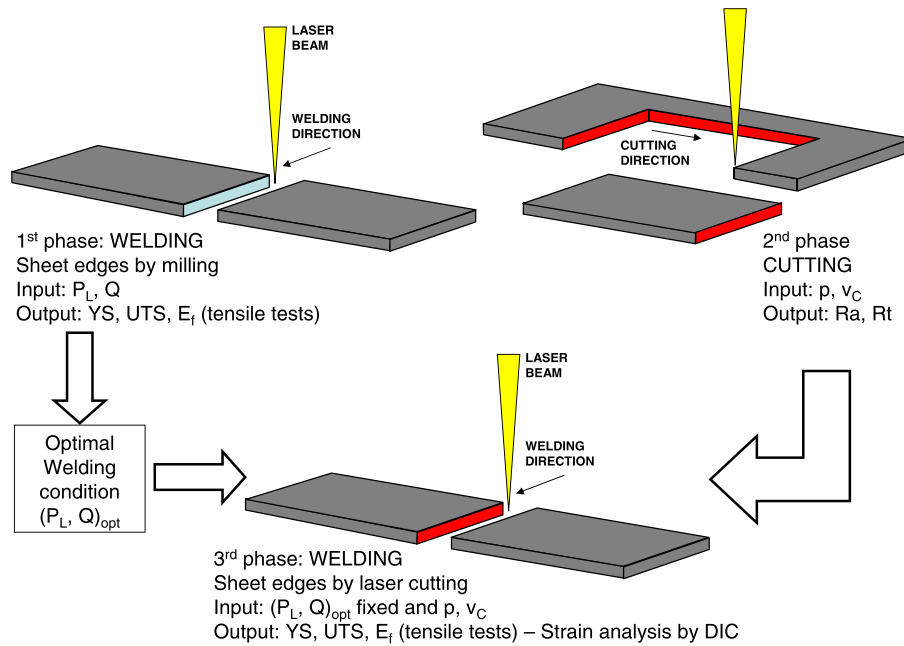
Fig. 1. Schematic representation of the experimental procedure.

search of optimal welding condition on machined edges by milling and the butt welding tests performed on sheets whose edges were obtained by laser cutting.

The welding equipment consisted in a TRUMPF HL2006D laser source equipped with a gantry system. The HL2006D is a Nd:YAG continuous wave laser with a 1.064 µm wavelength, with 2000 W as a maximum output power assured at the end of the optic chain. Laser beam is delivered to the focusing head by an optic fiber with 600 µm core diameter. A collimation lens of 200 mm and a focal lens of 150 mm were used to obtain a spot diameter size of 550 µm. The definition of the welding set-up and, in particular, of the focal point position and the configuration of the shielding gas system, derived on results available from preliminary bead on plate tests [51]. Appropriate strategies have been taken to shield the fusion zone and the heated surfaces until they are cooled below the reactivity temperature, since titanium is highly reactive with atmospheric elements (oxygen, nitrogen and hydrogen) at high temperatures. In particular a shielding trailer that covered an area of 30 mm × 300 mm was used. Argon was used as shielding gas for the both top side (flow rate of 40 Nl/min) and the bottom side of the weld (flow rate of 15 Nl/min). Helium was used for plasma gas suppression at a total flow rate of 20 Nl/min. Butt joints were made by welding on the short side plates of size 100 mm × 150 mm. Laser welding was performed along the specimen length, which is perpendicular to the rolling direction of the sheet material. Prior to clamp and weld the plates, the surfaces of the short side were cleaned with ethanol. The best welding operating condition was researched on sheets with machined edges within the following ranges of selected input parameters that identify the different welding conditions, indicated as Machined edges Welded Joint (MWJ). P_L and $Q = P_L/v_W$, were varied on two levels: 1000 W and 2000 W for P_L; 13 J/mm and 15 J/mm for Q. Within this range, the effect of power and heat input that leads to technological advantages and optimal values of mechanical properties was analyzed.

2.2. Laser cutting tests

The multimode fiber laser used for cutting experiments had the following specifications: 2 kW maximum output power, 1.07 µm

wavelength, 100 µm output fiber core diameter. The laser beam was focused using a 127 mm focal length lens. The spot diameter on surface was equal to 190 µm setting the focal point 0.5 mm above the sheet. Laser cutting tests were carried out in CW at 2000 W as power level, kept unchanged for all experimental trials.

The choice of the shear gas type used is fundamental [19]. For example air- and nitrogen-assisted laser cutting lower significantly the mechanical properties and corrosion resistance of titanium alloy. Thus, they are not suitable for applications with welding requirements due to the inclusions of titanium oxide and nitride. High-pressure cutting with a completely inert gas, is therefore the preferred method for the laser cutting of titanium and its alloys. In these experimental tests, argon was chosen as assist gas and it was supplied coaxially using a cylindrical copper nozzle with 2 mm exit diameter. A standoff distance of 0.5 mm from the workpiece was set.

Independent variables of the cutting tests were p and v_C. The selected input parameters were varied on two levels: 0.3 MPa and 0.6 MPa for p; 10 m/min and 20 m/min for v_C. In this case the different laser cutting conditions are indicated as Laser cut edges Welded Joints (LWJ) for the subsequent welding phase.

In a preliminary phase, for each cutting condition, five linear cuts of 50 mm length were made to asses the permanence of stable cutting conditions. After that, rectangular plates having the size 100 mm × 150 mm were cut in order to perform the next phase of the experimental activity. As indicators of the cutting edge quality, Ra and Rt were considered; such parameters were evaluated on the two short sides of the plates which would have been used for welding experiments. The surface roughness tester Mitutoyo Surftest SJ-401 (minimum resolution 0.000125 µm in 8 µm range) was used. In particular, roughness measurements were carried out in two locations of cut edges, the upper (UP) and the lower (LOW) part; they were made in accordance with the recommendations specified in the International Standard ISO 4288 [52].

2.3. Mechanical characterization and DIC techniques strain analysis

Uniaxial tensile tests were carried out on butt weld joints by means of a electromechanical universal testing machine Instron 4485 (maximum load: 200 kN; maximum test speed: 500 mm/

Fig. 2. Aramis 3-D digital image correlation system integrated on a INSTRON 4485 universal tensile testing machine.

(resolution 0.001 mm). Two samples for each condition were tested at room temperature using a 200 KN load cell, a 2620-603 Instron strain gauge extensometer (gauge length of 25 mm) and a constant crosshead speed of 3 mm/min. Data acquisition was made through computer using a specific Virtual Instrument created by LabVIEW (National Instruments). In this work, the ARAMIS 3D optical deformation analysis system developed by GOM Gmbh was used as DIC system. The experimental setup (see Fig. 2) allowed to obtain the full field strain maps by means of two cameras. The application of such method requires a surface treatment on the test samples: before testing, tensile specimens were prepared by applying a random black speckle pattern onto a matt white background previously applied on the gage length of the sample. In this way the data acquisition by DIC was enabled by the software that correlates the images captured at different stages during the tensile test and calculates the strain data at each stage. This method allows calculating the evolution of deformation fields in the observed area, from the very beginning of the test until the fracture of the sample, by associating pixels in the series of the images. Therefore it is possible to show the strain state of a surface, a line or a point, at a given instant of the test or its evolution over the time. In this work, in order to analyse the local strain behaviour of different specimen zones, the principal strain e_1 and e_2, respectively parallel and transverse with respect to longitudinal direction (LD) as defined in Fig. 3, were acquired by the software. It was thus possible to obtain the strain along the principal directions in the middle of the specimen width at different stages (the acquisition rate was 1 stage/s). Furthermore, the strain evolution over time for particular points, namely the failure point (FAIL), the point placed in the weld bead (WELD) and the point placed in the base material (BM) far from the failure, were analyzed. Strain behaviour of MWJ and LWJ specimens were compared in order to show the effect of cut edge quality on the strain behaviour.

3. Results and discussion

In this section the results obtained by the experiments are analyzed and discussed. This is done in three sub-sections: the first describes the best welding operating condition detection phase; in the next sub-section, results concerning the effect of cutting parameters on mechanical behaviour of butt joints are presented;
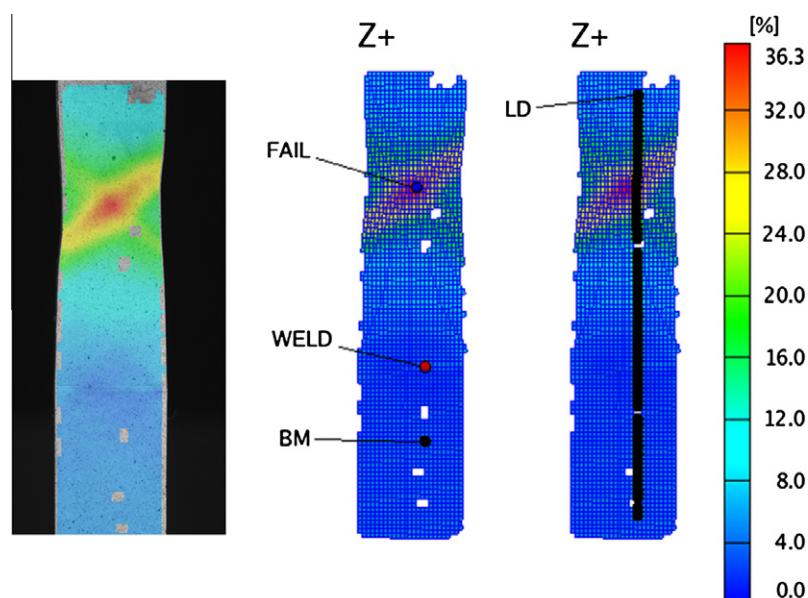
min). For mechanical characterization three output parameters, namely YS, UTS and E_f were considered when assessing the welded joints. Tensile dogbone specimens were machined by milling according to the ISO 6892-1 and ISO 4136 standards [53,54]; in particular a gauge length of 100 mm, a parallel length of 110 mm and an overall length of 240 mm were adopted. The specimen thickness was measured through a Mahr 40 EW digital micrometer
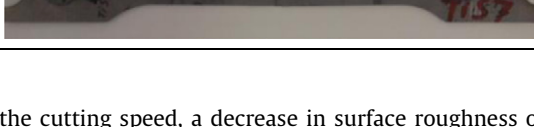

Fig. 3. Major strain field obtained in welded specimen by means of DIC techniques in the stage before the fracture.

Table 1
Tensile tests results (average values of two samples for each condition) and failure locations of tensile specimen tested for best welding operating condition detection phase (MWJ conditions).

ID	P_L, kW	Q, J/mm	v_W, m/min	$YS_{0.2\%}$, MPa	UTS, MPa	E_f	Failure location	Image
MWJ1	1	15	4.0	921.15	1043.8	0.078	Base material	
MWJ2	1	13	4.6	936.9	1094.9	0.097	Base material	
MWM3	2	15	8.0	838.6	968.4	0.059	Base material	
MWJ4	2	13	9.2	844.6	902.7	0.010	Weld bead	

in the third sub-section, the deformative behaviour of butt joints obtained with MWJ and LWJ conditions are compared.

3.1. Detection of best butt joint welding condition

The effect of P_L and Q on YS, UTS, E_f and on the failure location in the MWJ conditions is resumed in Table 1. It can be noted that only in the MWJ4 condition, that corresponds to the absolute highest cutting speed used, the fracture is located in the weld bead. For this reason this condition is rejected since it is far from the optimal welding condition. For the conditions MWJ1, MWJ2 and MWJ3 the failure occurs in the base material: in fact, as confirmed by Fig. 4, mechanical strength characteristics YS and UTS have similar values. For this reason, in order to select the optimal welding condition, technological considerations suggest that the condition with maximum power and maximum welding speed is the most advantageous.

In conclusion, mechanical characterization reveals that the optimal butt joint welding condition is identified as MWJ3, that corresponds to $P_L = 2$ kW and $Q = 15$ J/mm.

3.2. Effect of laser cutting parameters on cut edge quality

As regards the quality assessment of cutting edges in terms of Ra (Fig. 5), in the upper part of the cutting edge, the v_C and p effect is not negligible and Ra UP takes values between 0.55 μm and 1.36 μm. At the lower part of the cut edge, it can be noted that increasing the cutting speed, a decrease in surface roughness occurs. In this case the Ra LOW range is between 1.30 μm and 2.53 μm. Therefore the cut quality in terms of Ra is better at higher cutting speed and at the upper part of the cut edge. In particular for Ra LOW, p has not influence on the roughness at high values of v_C. When the v_C = 10 m/min, Ra increases his value of about 30% as result of halving the assist gas pressure from 0.6 MPa to 0.3 MPa. Concerning Rt UP trend (see Fig. 6), it is quite similar to Ra UP and values are in the range between 10.33 μm and 4.18 μm. Rt LOW values are in the range between 10.53 μm and 21.3 μm, and its trend is different with respect to Ra LOW. In fact, the influence of the assist gas pressure is important, unlike the effect of cutting speed that appears to be not significant. In particular, laser cuts made with $p = 0.3$ MPa, show values of Rt about 150% larger than the values obtained cutting at 0.6 MPa, independently from the value of the cutting speed.

A comparison with results reported in literature shows that obtained cuts can be considered superior in terms of both cutting speed value and cut edges quality. In fact, if compared with results by Rao et al. [19] using CO_2 laser in CW ($P_L = 600$ W) and Argon as assist gas ($p = 0.6$ MPa), a maximum cutting speed of about 0.9 m/min was obtained, much lower than the one reached in this work. In order to take into account the different laser power used, the comparison can be performed in terms of severance energy defined by Steen [56] as the ratio $P_L/(v_C * t)$. In case of titanium cut with Argon, the reported [56] average value for CW CO_2 laser cutting is 14 J/mm². In the present work severance energy is in the range
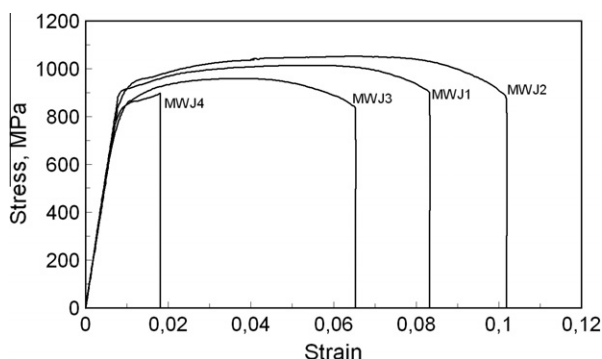

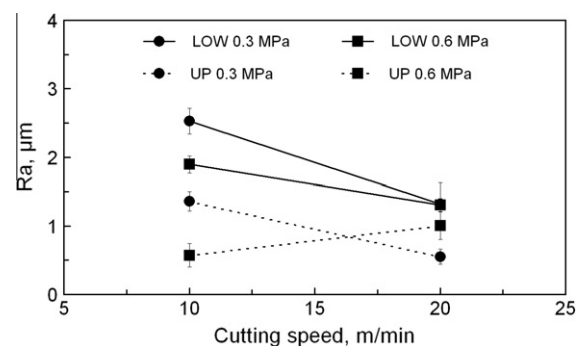**Fig. 4.** Engineering stress–strain diagrams for specimens in MWJ conditions.

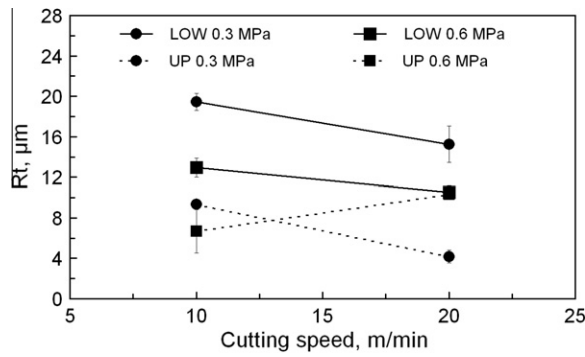**Fig. 5.** Influence of the cutting speed and assist gas pressure on Ra.

Fig. 6. Influence of the cutting speed and assist gas pressure on Rt.

Fig. 7. Engineering stress–strain diagrams for specimens in LWJ conditions.

between 6 and 12 J/mm^2 and it is lower than the value calculated starting from results reported by Rao et al. [19], equal to 40 J/mm^2. If compared with results obtained with Nd:YAG lasers, it can be noted that processing in PM reduces the maximum cutting speeds achievable in comparison to fiber laser operating in CW. In fact, experiments carried out with maximum cutting speeds equal to 0.18 m/min [16], 0.076 m/min [17], 0.824 m/min [18] and 0.025 m/min [7] can be found in literature. If considering the cut quality obtained in this work, it can be noted that the maximum value of roughness (Ra LOW = 2.53 μm), is lower than minimum values reported in comparable experimental work. In particular, Almeida et al. [18] obtained the minimum Ra of 2.67 μm and Pandey and Dubey [7] reported Ra equal to about 6.95 μm corresponding to the optimum level of control factors that minimize the surface roughness characteristics.

It can be concluded that, in absolute terms, the highest values of roughness are obtained on the lower part of the cutting edge; in particular differences in processing conditions are much more evident on the Rt parameter. Results of cut edge quality obtained by laser cutting have to be compared with the edge quality of parts obtained by milling. In this case values of Ra and Rt measured, were equal to 0.24 μm and 1.8 μm, respectively.

3.3. Effect of laser cutting parameters on butt joints mechanical behaviour

Results from tensile tests performed on butt joints obtained with LWJ conditions, detailed in Table 2, are now presented and
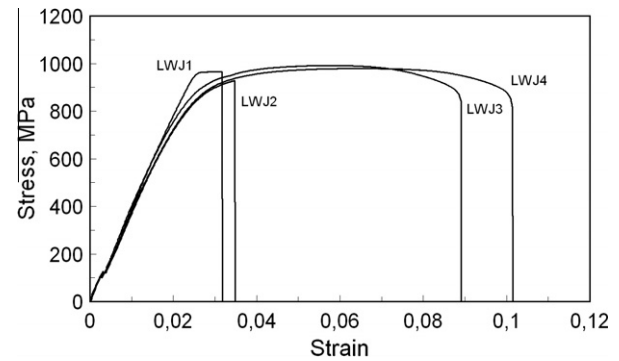
compared with MWJ3. All these specimens are welded using the same (optimal) welding condition (P_L = 2 kW; Q = 15 J/mm).

As it can be seen from Fig. 7, the stress–strain curves showed that in two of the four investigated conditions (LWJ1 and LWJ2), the fracture occurred very close to the yielding point, at the beginning of the plastic field. In such conditions the failure occurs in the weld bead. The strength differences recorded in all tests are negligible (see Table 2). The average values of UTS are in the range 992–972 MPa for LWJ3 and LWJ4 conditions (failure in the base material), and in the range 965–926 MPa for LWJ1 and LWJ2 conditions. Greater differences are observed for E_f since it takes values in the range 0.003–0.102 (if considering all tests, including replications). The minimum average value of E_f value corresponds to the LWJ1 condition, whereas the maximum average value of E_f is obtained in the LWJ4 condition, as it can be seen in Table 2.

It can be observed that the cutting speed has almost negligible influence, unlike gas pressure. In fact, the tensile specimen images in Table 2 clearly show that the two conditions in which the fracture occurs in the weld bead, namely LWJ1 and LWJ2, are those obtained using plates cut setting p = 0.3 MPa. On the contrary, tensile specimens that show the best results in terms of mechanical properties, are those obtained with LWJ3 and LWJ4 conditions. These specimens have edges cut setting p = 0.6 MPa and show the lowest values of roughness (in particular Rt) at the lower part of the cut edge, as reported in the Section 3.2. These results show that the assist gas pressure plays a fundamental role in creating defects that worsen the mechanical behavior of the welded joints, because they affect the cut edge quality. This is because it

Table 2
Tensile tests results (average values of two samples for each condition) and failure locations of tensile specimen tested for investigation of cutting parameters effect on mechanical behaviour of butt joints (LWJ conditions).

ID	p, MPa	v_C, m/min	$YS_{0.2\%}$, MPa	UTS, MPa	E_f	Failure location	Image
LWJ1	0.3	10	962.9	965.1	0.005	Weld bead	
LWJ2	0.3	20	798.1	925.6	0.012	Weld bead	
LWJ3	0.6	10	865.7	991.8	0.069	Base material	
LWJ4	0.6	20	822.3	972.1	0.090	Base material	

influences the quality of laser cutting edges, that allows obtaining sound welds in the next manufacturing step.

The effect of changing the cut edge quality due to the variation of process parameters (p and v_C) or the adoption of different manufacturing process (laser cutting VS milling) can be investigated by the comparative analysis of local deformations performed by DIC techniques, as reported in the following section.

3.4. Comparative strain analysis

Figs. 8 and 9 show the comparison of the strain along the LD direction. In particular, Fig. 8 compares the major strain in the LD section of specimens in different conditions at the same stage (i.e. the stage just before the failure of the specimen in LWJ1 condition). As it can be seen from Fig. 7, in this stage all specimens are in plastic field. Fig. 8 shows a similar deformative behaviour between LWJ conditions. Only in the LWJ1 condition it can be noted a slight increase of major strain in one part of the specimen. Fig. 8 also shows that the specimen in MWJ3 condition has an early and noticeable localization of strain in the base material. In case of tests in which the fracture occurred in the weld bead (LWJ1 and LWJ2 conditions), the early fracture occurs due to the defects on the surface of the weld bead. Fig. 8 shows absolute values of e_1 and e_2 equal to 2.43% and 1.19%, respectively. These values are lower than the ones of tests performed in MWJ3, LWJ3 and LWJ4 conditions, as it is possible to highlight in Fig. 9, where data are reported in the stage just before the corresponding failure. In fact, specimens in LWJ3 and LWJ4 conditions, exhibit absolute values of e_1 and e_2 equal to about 52% and 24%, respectively. Such values are similar to those obtained by MWJ3 specimen (e_1 = 49.4%, e_2 = 23%) since the base material is the same. From Fig. 9 it can be also seen that, with reference to the weld line that divides the specimen into two parts, the strain is localized in one side only. The weld bead thus represents a constraint that leads to the strain localization and the subsequent failure in one side only, while in the other side the strain remains at low values.

This effect of the weld bead on the deformative behaviour of specimen can be also highlighted observing the trend of strain over time in different points (Figs. 10 and 11). Fig. 10 shows the major strain evolution in the point where the strain localizes (and thus the failure occurs): the specimen in MWJ3 condition fails before than LWJ3 and LWJ4. This is due to the early localization of strain in one side of specimen (as shown in Fig. 8) that reduces both the time in which the fracture occurs and the strain contribution in the other side of specimen: the lower this contribution, the lowest the time of the test before fracture. In addition, the differences between LWJ and MWJ3 conditions are evident from the beginning of tensile tests since, as illustrated in Fig. 10, the specimen in MWJ3 condition has a steeper increase of strain over time.
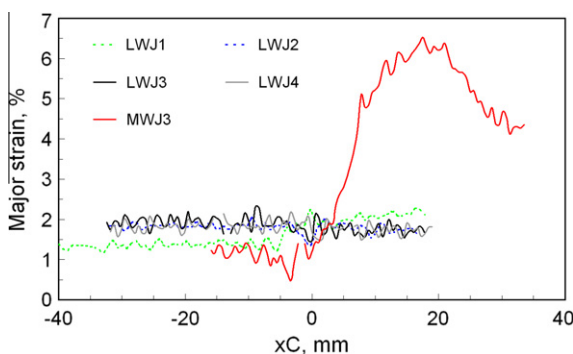

Fig. 9. Major (solid line) and Minor (dashed line) strain as a function of distance from the center of the weld bead in the LD direction. Data recorded for MWJ3 (117), LWJ3 (174) and LWJ4 (199) in the stage just before the failure. Number in brackets indicates the failure stage.
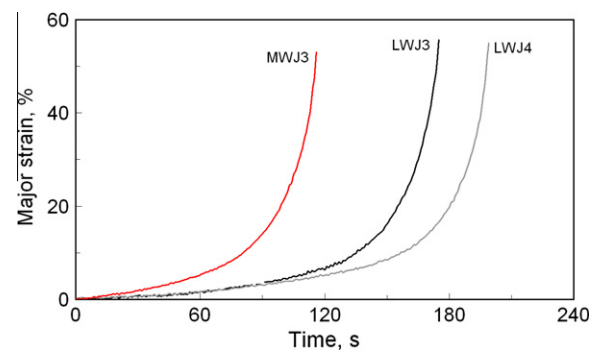
Fig. 10. Major strain trends over time of points (FAIL) where the failure occurs. Comparison of MWJ optimal condition and LWJ specimen with failure in base material.
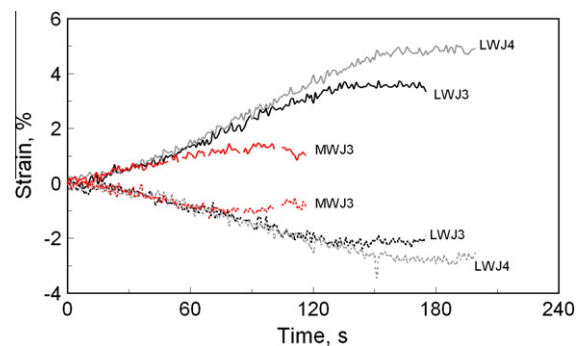
Fig. 11. Major (solid line) and minor (dashed line) strain trends over time of points (WELD) in the weld bead. Comparison of MWJ optimal condition and LWJ specimen with failure in base material.

The optimal values of cutting process parameters are represented by LWJ4 condition obtained setting assist gas pressure equal to 0.6 MPa and cutting speed equal to 20 m/min. This because the fracture occurs later (Fig. 10) and E_f is higher (Fig. 7). Furthermore Fig. 10 confirms that in the last stage the same values of e_1 are reached by MWJ3, LWJ3 and LWJ4. The trends are similar for e_2 but are not represented here.

In order to highlight this behaviour, strain of WELD points is illustrated in Fig. 11. It can be noted the much lower e_1 values with respect to FAIL points (Fig. 10). Fig. 11 shows that strain of specimen in MWJ3 condition has absolute values lower than LWJ3 and LWJ4. The different deformative behaviour of specimens

Fig. 8. Major strain as a function of distance from the center of the weld bead in the LD direction at the same time. Data recorded for all specimens in the stage just before the LWJ1 specimen failure.
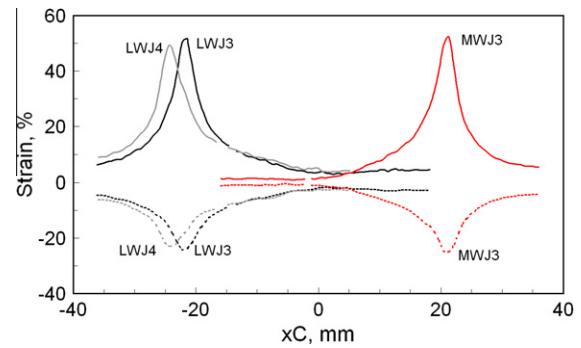
in MWJ and LWJ conditions, may be explained by the different gap resulting from the cut edges quality that in turn depends from one side on the laser process parameters used and from the other side on the manufacturing approach. In the first case, the possible effect of the change in cut edge quality and in particular of the Rt increase, is to exceed an upper limit and thus a critical gap distance for achieving sound welds that worsen the mechanical properties of the joint and lead to an early fracture in the weld. From the other side, experimental results show that lower values of gap influence the weld bead mechanical behaviour resulting in a limit for achieving higher values of strain. In fact, milling process allows to obtain the lowest value of roughness and thus narrow gap in the sheet clamping phase. Moving from a value of gap near to zero (MWJ3) towards the one obtained by combining sheets cut by laser proper parameters (LWJ3, LWJ4) the strain in the weld bead points (WELD) increases by about 4%, as it can be seen in Fig. 11. These results are completely in accordance with the tensile behaviour of laser welded Ti6Al4V 3 mm thick sheets reported by Cao et al. [33]. The most important points of agreement are: (i) the significant effect of the gap between the sheet edges on the elongation to fracture and strength characteristics of joints and the experimental evidence (supported by strain analysis using DIC techniques); (ii) the existence of an optimal range of gap values able to obtain optimal joint mechanical performances. In fact, experiments carried out by Cao et al. [33] show that the optimal tensile properties are obtained at an intermediary joint gap that is approximately 10% of the material thickness (0.2–0.3 mm). The explanation given by Cao et al. is based on the examination of weld integrity and microstructure by means of optical microscopy; it was not related to the change in weld bead deformative behaviour and thus to the strain localization in one side of the specimen, as it could be deduced in this work using the DIC system.

Concerning the critical gap distance, a general rule sets the maximum fitup gap less than 5% of the thickness [55]. The critical gap value obtained by experimental results in this work seems to be narrower than 5% of the thickness. In fact, welds with failure in weld bead occurs for a gap distance smaller than 50 μm, in the hypothesis that gap distance is roughly equivalent to the sum of the maximum values of Rt obtained. In this case, the best joint gap is approximately 2.5% of the material thickness. These results are in agreement with experimental results reported by Bagger et al. [31]: for 1.8 mm thick steel sheets, edges with squareness in range 0.015–0.040 μm well suited to subsequent laser weld and thus to manufacture tailored blanks, were obtained. In addition, in the same work, it was also reported the influence of laser power on the critical gap distance: to achieve sound welds, gap has to be kept as small as 0.05 mm (valid for 1500 W CO_2 laser) and could be larger up to 0.15 mm if laser power is increased up to 3000 W. Different experimental findings were reported by Cao et al. [33] where the best joint gap is approximately 10% of the material thickness and the maximum gap tolerance was determined to be about 16% of material thickness that is approximately corresponds to the spot size used.

Concerning the feasibility of performing the direct weld of thin sheets blanks based on laser cutting–welding combination process, results obtained in this work for Ti alloys are in accordance with ones reported by Wang et al. [32] for zinc-coated sheets of the same thickness: also in this case, controlling the quality of laser cutting represents the most important factor, along with the sheet flatness and gap between (<0.05 mm) the sheets, to achieve sounds welds.

4. Conclusions

The present investigation primarily shows the feasibility of achieving modern sustainability requirements (like weight reduc-tion) by the laser cutting-welding combination, which reduces machining cost and allows the titanium alloys usage optimization. In fact, the correct selection of fiber laser cutting parameters allows to obtain parts with edges well suited for subsequent direct laser welding (welds are in fact characterised by mechanical properties comparable with ones obtained by milling) without the need for further edge machining.

In particular, the experimental activity carried out in this work allowed to highlight the following main effects of the fiber laser cutting parameters (the cutting speed and the assist gas pressure) on mechanical properties and strain behaviour of 1 mm Ti6Al4V butt joints whose edges were prepared by fiber laser cutting:

- Cuts performed with the lowest value of assist gas pressure equal to 0.3 MPa show failure in the weld bead. In such a process condition, high roughness values (Rt) could be detected on the cutting edges. The exceeding of a critical gap distance was thus associated to the failure.
- Comparative strain analysis performed by a digital image correlation technique reveals difference between specimens with milling machined edges and specimens whose edges were obtained varying the laser cutting parameters: in fact, the narrow gap resulting from the reduced cut edge roughness obtained by milling, influences the mechanical behaviour of the weld bead and limits the strain in one part of the specimen.
- The cutting condition most suitable for the subsequent laser welding is characterised by the assist gas pressure value of 0.6 MPa and the cutting speed of 20 m/min, since in the tensile specimens obtained using such a process condition, the failure occurred in the base material.

Additional experimental investigations about controlled gap influence on mechanical properties of welded joints are necessary. Investigation about the influence on joint mechanical properties as a result of variations in weld bead geometry and changes in microstructure of Ti6Al4V due to laser cutting and subsequent welding are needed. Furthermore, it is highly desirable to focus future studies also on investigation of the aptitude of laser butt welding Ti6Al4V thin sheets whose edges were prepared by fiber laser cutting, to plastic deformation and superplastic forming by means of bending, stamping and blow forming tests.

References

[1] Mayyas A, Qattawi A, Omar M, Shan D. Design for sustainability in automotive industry: a comprehensive review. Renew Sust Energy Rev 2012;16:1845–62.
[2] Palumbo G, Sorgente D, Tricarico L. The design of a formability test in warm conditions for an AZ31 magnesium alloy avoiding friction and strain rate effects. Int J Mach Tool Manu 2008;48:1535–45.
[3] Cui X, Zhang H, Wang S, Zhang L, Ko J. Design of lightweight multi-material automotive bodies using new material performance indices of thin-walled beams for the material selection with crashworthiness consideration. Mater Design 2011;32:815–21.
[4] Palumbo G, Sorgente D, Tricarico L. Numerical-experimental analysis of thin magnesium alloy stripes subjected to stretch-bending. J Mater Process Technol 2008;201:183–8.
[5] Meshram SD, Mohandas T. A comparative evaluation of friction and electron beam welds of near-a titanium alloy. Mater Design 2010;31:2245–52.
[6] Norgate TE, Jahanshahi S, Rankin WJ. Assessing the environmental impact of metal production processes. J Clean Prod 2007;15:838–48.
[7] Pandey AK, Dubey AK. Simultaneous optimization of multiple quality characteristics in laser cutting of titanium alloy sheet. Opt Laser Technol 2012;44:1858–65.

[8] Mueller S, Bratt C, Mueller P, Cuddy J, Shankar K. Laser beam welding of titanium – a comparison of CO_2 and fiber laser for potential aerospace applications. In: Proceedings of the ICALEO; 2008. p. 846–54.

[9] Blackburn J, Allen C, Hilton P, Li L. Nd:YAG Laser welding of titanium alloys using a directed gas jet. J Laser Appl 2010;22(2):71–8.

[10] Abbasi M, Ketabchi M, Labudde T, Prahl U, Bleck W. New attempt to wrinkling behavior analysis of tailor welded blanks during the deep drawing process. Mater Design 2012;40:407–14.

[11] Mohebbi MS, Akbarzadeh A. Prediction of formability of tailor welded blanks by modification of MK model. Int J Mech Sci 2012;61(1):44–51.

[12] Lai CP, Chan LC, Chow CL. Effects of tooling temperatures on formability of titanium TWBs at elevated temperatures. J Mater Process Technol 2007;191:157–60.

[13] Chan LC, Lai CP, Chow CL, Cheng CH. Experimental approach on stress–strain analysis of weldment in Ti-TWBs at elevated temperatures. Int J Adv Manuf Technol 2009;40:470–7.

[14] Qiu XG, Chen WL. The study on numerical simulation of the laser tailor welded blanks stamping. J Mater Process Technol 2007;187–188:128–31.

[15] Davim JP, editor. Lasers in Manufacturing. London: ISTE-Wiley; 2012, ISBN 978-1-84821-369-2.

[16] Lv Shanjin. Yang W. An investigation of pulsed laser cutting of titanium alloy sheet. Opt Lasers Eng 2006;44:1067–77.

[17] Chien WT, Hung WC. Investigation on the predictive model for burr in laser cutting titanium alloy. Mater Sci Forum 2006;526:133–8.

[18] Almeida IA, de Rossi W, Lima MSF, Berretta JR, Nogueira GEC, Wetter NU, et al. Optimization of titanium cutting by factorial analysis of the pulsed Nd:YAG laser parameters. J Mater Process Technol 2006;179:105–10.

[19] Rao BT, Kaul R, Tiwari P, Nath AK. Inert gas cutting of titanium sheet with pulsed mode CO_2 laser. Opt Lasers Eng 2005;43:1330–48.

[20] Scintilla LD, Sorgente D, Tricarico L. Experimental investigation on fiber laser cutting of Ti6Al4V thin sheet. Adv Mater Res 2011;264–265:1281–6.

[21] Wandera C, Kujanpää V. Characterization of the melt removal rate in laser cutting of thick-section stainless steel. J Laser Appl 2010;22:62–70.

[22] Olsen FO. Laser cutting from CO_2 laser to disc or fiber laser – possibilities and challenges. In: Proceedings of ICALEO; 2011. p. 6–15.

[23] Petring D, Schneider F, Wolf N. Some answers to frequently asked questions of laser beam cutting. In: Proceedings of ICALEO; 2012. p. 43–48.

[24] Hirano K, Fabbro R. Possible explanations for different surface quality in laser cutting with 1 and 10 μm beams. J Laser Appl 2012; 24: 012006 1–8.

[25] Scintilla LD, Tricarico L. Estimating cutting front temperature difference in disk and CO_2 laser beam fusion cutting. Opt Laser Technol 2012;44:1468–79.

[26] Scintilla LD, Tricarico L. Experimental investigation on fiber and CO_2 inert gas fusion cutting of AZ31 magnesium alloy sheets. Opt Laser Technol 2013;46:42–52.

[27] Scintilla LD, Tricarico L, Mahrle A, Wetzig A, Beyer E. A comparative study of cut front profiles and absorptivity behavior for disk and CO_2 laser beam inert gas fusion cutting. J Laser Appl 2012;24(5):052006.

[28] Powell J, Kaplan A.F.H. A technical and commercial comparison of fiber laser and CO_2 laser cutting. In: Proceedings of ICALEO; 2012. p. 277–281.

[29] Gasner I. Laser triming of hot formed steels: a comparison between 10,6 and 1 μm laser light. In: Proceedings of the ICALEO; 2010. p. 277–80.

[30] Schneider F, Petring D. Flexible 3D – laser cutting and welding with the combi-head. In: Proceedings of ICALEO; 2008. p. 582–88.

[31] Bagger C, Olsen FO. Pulsed mode laser cutting of sheets for tailored blanks. J Mater Process Technol 2001;115:131–5.

[32] Wang C, Hu L, Liu J, Hu X, Du H. Joint performance for laser cutting-welding of zinc-coated tailored blanks. J Wuhan Univ Technol 2005;20:46–9.

[33] Cao X, Debaecker G, Poirier E, Marya S, Cuddy J, Birur A, Wanjara P. Tolerances of joint gaps in Nd:YAG laser welded Ti-6Al-4V alloy with the addition of filler wire. J Laser Appl 2011; 23 1: 012004 1–10.

[34] Gao XL, Zhang LJ, Liu J, Zhang JX. A comparative study of pulsed Nd:YAG laser welding and TIG welding of thin Ti6Al4V titanium alloy plate. Mat Sci Eng A-Struct 2013;559:14–21.

[35] Kabir ASH, Cao X, Baradari JG, Wanjara P, Cuddy J, Birur A, et al. Determination of global and local tensile behaviours of laser welded Ti-6Al-4V alloy. Adv Mater Res 2012;409:859–64.

[36] Kabir ASH, Cao X, Gholipour J, Wanjara P, Cuddy J, Birur A, et al. Effect of postweld heat treatment on microstructure, hardness, and tensile properties of laser-welded Ti-6Al-4V. Metal Mater Trans A 2012;43:4171–84.

[37] Cao X, Jahazi M. Effect of welding speed on butt joint quality of Ti6Al4V alloy welded using a high-power Nd:YAG laser. Opt Lasers Eng 2009;47:1231–41.

[38] Blackburn JE, Allen CM, Hilton PA, Li L, Hoque MI, Khan AH. Modulated Nd:YAG laser welding of Ti–6Al–4V. Sci Technol Weld Joi 2010;15(5):433–9.

[39] Casalino G, Curcio F. Memola Capece Minutolo F. Investigation on Ti6Al4V laser welding using statistical and Taguchi approaches. J Mater Process Technol 2005;167:422–8.

[40] Anand D, Chen DL, Bhole SD, Andreychuk P, Boudreau G. Fatigue behavior of tailor (laser)-welded blanks for automotive applications. Mat Sci Eng A-Struct 2006;420:199–207.

[41] Reisgen U, Schleser M, Mokrov O, Ahmed E. Optimization of laser welding of DP/TRIP steel sheets using statistical approach. Opt Laser Technol 2012;44:255–62.

[42] Genevois C, Deschamps A, Vacher P. Comparative study on local and global mechanical properties of 2024 T351, 2024 T6 and 5251 O friction stir welds. Mater Sci Eng A – Struct 2006;415:162–70.

[43] Hatamleh O. Effects of peening on mechanical properties in friction stir welded 2195 aluminum alloy joints. Mater Sci Eng A 2008;492:168–76.

[44] Brown R, Tang W, Reynolds AP. Multi-pass friction stir welding in alloy 7050–T7451: effects on weld response variables and on weld properties. Mater Sci Eng A 2009;513–514:115–21.

[45] Leitão C, Galvão I, Leal RM, Rodrigues DM. Determination of local constitutive properties of aluminium friction stir welds using digital image correlation. Mater Design 2012;33:69–74.

[46] Zadpoor AA, Sinke J, Benedictus R. Finite element modeling and failure prediction of friction stir welded blanks. Mater Des 2009;30:1423–34.

[47] Nielsen KL, Pardoen T, Tvergaard V, de Meester B, Simar A. Modelling of plastic flow localisation and damage development in friction stir welded 6005 A aluminium alloy using physics based strain hardening law. Int J Solids Struct 2010;47:2359–70.

[48] Lockwood WD, Reynolds AP. Simulation of the global response of a friction stir weld using local constitutive behaviour. Mater Sci Eng A 2003;339:35–42.

[49] Boyce B, Reu P, Robino C. The constitutive behavior of laser welds in 304 L stainless steel determined by digital image correlation. Metal Mater Trans A 2006;37:2481–92.

[50] Scintilla LD, Tricarico L, Brandizzi M, Satriano AA. Nd:YAG laser weldability and mechanical properties of AZ31 magnesium alloy butt joints. J Mater Process Technol 2010;210:2206–14.

[51] Scintilla LD, Sorgente D, Palumbo G, Tricarico L, Brandizzi M, Satriano AA. Influence of fiber laser cutting parameters on the subsequent laser weding of Ti6Al4V sheets. In: Proceedings of ICALEO; 2011. p. 25–33.

[52] International Standard ISO 4288:1996, Geometrical Product Specifications (GPS) – Surface texture: Profile method – Rules and procedures for the assessment of surface texture.

[53] International Standard ISO 6892–1:2009. Metallic materials – tensile testing – Part 1: Method of test at room temperature.

[54] International Standard ISO 4136:2001. Destructive tests on welds in metallic materials – transverse tensile test.

[55] Ready JF. LIA handbook of laser materials processing. Orlando, FL, USA: Laser Institute of America Magnolia Publishing Inc.; 2001.

[56] Steen WM. Laser material processing. 3rd ed. NewYork: Springer; 1991.